THE JOURNAL OF BIOLOGICAL CHEMISTRY VOL. 286, NO. 2, pp. 1609–1617, January 14, 2011

Characterization of a *Listeria monocytogenes* Ca^{2+} Pump

A SERCA-TYPE ATPase WITH ONLY ONE Ca^{2+}-BINDING SITE[*][S]

Received for publication, August 19, 2010, and in revised form, October 21, 2010 Published, JBC Papers in Press, November 3, 2010, DOI 10.1074/jbc.M110.176784

Kristina Faxén[‡1,2], Jacob Lauwring Andersen[‡1], Pontus Gourdon[‡], Natalya Fedosova[§], Jens Preben Morth[‡3], Poul Nissen[‡4], and Jesper Vuust Møller[§5]

From the Departments of [‡]Molecular Biology, Gustav Wieds Vej 10C, and [§]Physiology and Biophysics, Ole Worms Allé 6, Centre for Membrane Pumps in Cells and Disease, PUMPKIN, Danish National Research Foundation, Aarhus University, DK-8000, Aarhus, Denmark

We have characterized a putative Ca^{2+}-ATPase from the pathogenic bacterium *Listeria monocytogenes* with the locus tag *lmo0841*. The purified and detergent-solubilized protein, which we have named *Listeria monocytogenes* Ca^{2+}-ATPase 1 (LMCA1), performs a Ca^{2+}-dependent ATP hydrolysis and actively transports Ca^{2+} after reconstitution in dioleoylphosphatidyl-choline vesicles. Despite a high sequence similarity to the sarcoplasmic reticulum Ca^{2+}-ATPase (SERCA1a) and plasma membrane Ca^{2+}-ATPase (PMCA), LMCA1 exhibits important biochemical differences such as a low Ca^{2+} affinity ($K_{0.5}$ ~80 μM) and a high pH optimum (pH ~9). Mutational studies indicate that the unusually high pH optimum can be partially ascribed to the presence of an arginine residue (Arg-795), corresponding in sequence alignments to the Glu-908 position at Ca^{2+} binding site I of rabbit SERCA1a, but probably with an exposed position in LMCA1. The arginine is characteristic of a large group of putative bacterial Ca^{2+}-ATPases. Moreover, we demonstrate that H^+ is countertransported with a transport stoichiometry of 1 Ca^{2+} out and 1 H^+ in per ATP hydrolyzed. The ATPase may serve an important function by removing Ca^{2+} from the microorganism in environmental conditions when *e.g.* stressed by high Ca^{2+} and alkaline pH.

The vital importance of maintaining Ca^{2+} homeostasis is well established. Whereas the Ca^{2+} levels in eukaryotes are kept under tight control, close to 1–3 mM in the blood plasma and around 50–150 nM in the cytoplasm, much less is known about the role of Ca^{2+} in prokaryotes (1). However, it has been found that in most bacterial cell types studied, Ca^{2+} levels are maintained in the micromolar range or lower by a variety of secondary and primary transporters such as P-type ATPases (2).

The P-type ATPases are integral, multispanning membrane proteins involved in the active transport of mainly cations across the membrane. The hallmark of the family is the formation of a high-energy phosphoenzyme intermediate targeting a conserved aspartate side chain. The Ca^{2+}-transporting P-type ATPases in eukaryotes belong to the subfamily II (3), including sarcoplasmic reticulum Ca^{2+}-ATPase (SERCA)[6] and the plasma membrane Ca^{2+}-ATPase (PMCA), corresponding to subgroups IIA and IIB, respectively. Despite a plethora of prokaryotic P-type ATPase genes acquired from bacterial genome sequences, very little is known about the biochemical function and *in vivo* importance of these pumps. Phosphorylation and Ca^{2+} transport has been documented in a few cases (4–8). It has also recently been shown that CaxP, a P-type ATPase in *Streptococcus pneumoniae*, is vital for the survival of this microorganism in the high extracellular Ca^{2+} concentrations of the infected host (9).

From an initial analysis of bacterial sequences we identified a number of putative Ca^{2+} pumps that although similar to eukaryotic Ca^{2+}-ATPases also differ from these, especially with respect to the region known as the Ca^{2+}-binding site I in SERCA (10–12). The presence of an arginine residue in the position corresponding to Glu-908 in SERCA1a, and the absence of an acidic residue corresponding to Glu-771 in SERCA1a, indicates that in this bacterial subgroup of Ca^{2+}-ATPases the site I region is not adapted for Ca^{2+} binding, as is also the case in PMCA (13, 14). However, in most other respects these bacterial ATPases retain more similarity with SERCA than with PMCA (described below). As a common feature, all sequences indicate the presence of a cation binding site in the region corresponding to site II in SERCA, centered on Glu-309 of the conserved PEGL motif found in all eukaryotic Ca^{2+}-ATPases.

In the present work, we focus on the biochemical and biophysical properties of a bacterial P-type ATPases, *lmo0841*, present in the pathogenic bacterium *Listeria monocytogenes* that is up-regulated during adaptation to alkaline pH (15). After having expressed and purified the gene product of *lmo0841* we show that indeed it has Ca^{2+}-dependent ATPase activity and transports Ca^{2+}. On this background we from now on refer to it as the *L. monocytogenes* Ca^{2+}-ATPase 1 (LMCA1). We characterize the ATPase activity, apparent Ca^{2+} affinity and Ca^{2+} transport as a function of pH. We es-

* This work was supported by a Center of Excellence grant from the Danish National Research Foundation, a post-doctoral fellowship from The Swedish Research Council (to P. G.), and a Hallas-Møller research stipend from the Novo Nordisk Foundation (to P. N.).

[S] The on-line version of this article (available at http://www.jbc.org) contains supplemental Figs. S1 and S2.

[1] Both authors contributed equally to this work.
[2] Present address: Department of Plant Biology and Biotechnology, Faculty of Life Sciences, University of Copenhagen, DK-1870 Frederiksbjerg C.
[3] Present address: The Biotechnology Centre of Oslo and Centre for Molecular Medicine, Nordic EMBL Partnership, University of Oslo, Oslo, Norway.
[4] To whom correspondence may be addressed. E-mail: pn@mb.au.dk.
[5] To whom correspondence may be addressed. E-mail: jvm@biophys.au.dk.

[6] The abbreviations used are: SERCA, sarcoplasmic reticulum Ca^{2+}-ATPase; LMCA1, *Listeria monocytogenes* Ca^{2+}-ATPase 1; β-OG, β-octylglucoside; C12E8, octaethylene glycol monododecyl ether; DDM, *n*-dodecyl β-D-maltoside; DOPC, dioleoyl phosphatidylcholine; PDB, Protein Data Bank; PMCA, plasma membrane Ca^{2+}-ATPase; TEV, Tobacco Etch Virus.

tablish for the first time H^+ counter transport as a feature of a bacterial P-type ATPase. Furthermore we demonstrate that the Ca^{2+} transport is electrogenic, with a probable 1 ATP:1 Ca^{2+}:1 H^+ stoichiometry. With the help of mutational studies we investigate the molecular basis for the biochemical characteristics of LMCA1 distinct from SERCA1a. Finally we explain how these differences can be rationalized from a homology model using SERCA1a as a template.

EXPERIMENTAL PROCEDURES

Cloning—The ORF of *lmo0841* (LMCA1) was amplified from *L. monocytogenes* genomic DNA with the primers *lmo0841*for: gcccatatggagatataccgcaaaagcgcg and *lmo0841*rev: gcccctcgaggccctgaaaataaagattctcagtagtggggatgtcgtaatctttgaaaaacttattctgaactactttaataat. The reverse primer was designed to incorporate a short linker, a Tobacco Etch Virus (TEV) protease site and a six histidine tag in the C terminus of the expressed enzyme. The PCR product was digested with NdeI and XhoI and ligated into pET-22b (Novagen) resulting in LMCA1-pET22-b.

Expression—LMCA1-pET-22b was transformed into C43 (DE3) and plated on lysogeny broth (LB) agar plates supplemented with 100 μg/ml ampicillin (amp). 5–10 colonies were used for inoculation of a 20-ml LB overnight culture with 100 μg/ml amp. 2 liters of terrific broth (TB) medium, supplemented with 100 μg/ml amp, was inoculated with 20 ml of overnight culture and grown at 30 °C. Expression was induced at $A_{600\,nm} = 0.6-0.8$ with 1 mM isopropyl β-D-1-thiogalactopyranoside (IPTG), and the temperature was lowered to 20 °C for induction for 20 h. 20 g of cells from 2 liters of medium were harvested by centrifugation at 5,000 × *g* for 45 min, resuspended in 100 ml buffer A (50 mM Tris-HCl, 200 mM KCl, 20% v/v glycerol, pH 7.6) and stored at −20 °C.

Purification—20 g of cells were lysed with a high pressure homogenizer (C5 model, Avestin) at 15,000 psi three times in 100 ml of buffer A supplemented with 5 mM β-mercaptoethanol, 1 mM PMSF, 1 Complete tablet (Roche), and 5 μg/ml DNase I. Cell debris and aggregates were removed by centrifugation at 27,000 × *g* for 30 min. A total of 2.7 g of mixed membranes were isolated by centrifugation at 235,000 × *g* for 2 h. The mixed membranes were solubilized in 50 ml of buffer B (20 mM Tris-HCl, pH 7.6, 200 mM KCl, 20% v/v glycerol, 5 mM β-mercaptoethanol, 3 mM $MgCl_2$, 0.1 mM $CaCl_2$) with 1% w/v β-dodecylmaltoside at 4 °C for 1 h. Aggregates were removed by centrifugation at 235,000 × *g* for 1 h. 4 ml of Ni-slurry (Ni-Sepharose 6 Fast Flow, GE Healthcare) was equilibrated in buffer C (20 mM MOPS pH 7.5, 200 mM KCl, 20% v/v glycerol, 5 mM β-mercaptoethanol, 1 mM $MgCl_2$, 0.1 mM $CaCl_2$, 0.25 mg/ml $C_{12}E_8$ (~6.6 × CMC)). Solubilized membranes were incubated with Ni-beads for 1 h, and the slurry was packed into a XK-16 column (GE Healthcare). 4 mg of protein was eluted in a single step in 20 ml of buffer C supplemented with 250 mM imidazole and was digested with 0.25 mg of TEV protease while dialyzing against 1 liter of buffer C. Digested and dialyzed LMCA1 was loaded on the Ni column, and the flow-through was collected yielding a pure sample (Fig. 1*A*).

Homology Modeling—To model LMCA1 in the calcium-bound E1P-ADP state and the extracellular-facing E2P ground state PDB ID entries 1T5T and 3B9B were used respectively as templates structures in MODELLER (16). For each template 100 models were generated, and the one with the lowest DOPE (Discrete Optimized Protein Energy) score (17) was used for further analysis.

SERCA1a Preparation—Sarcoplasmic reticulum vesicles were isolated from rabbit skeletal muscle and purified by extraction with a low concentration of deoxycholate as previously described (18).

Enzymatic Activity—Spectrophotometric measurements, using an ATP regenerating and NADH-coupled activity assay were performed, as described (19). The medium contained 10% glycerol, 10 mM bis-Tris propane, 150 mM KCl, 1 mM $MgCl_2$, 0.2 mM $NaMoO_4$, 5 mM NaN_3, with or without 20 mM KNO_3 at pH 7–7.5. The three latter substances were added as inhibitors of phosphatases, F_1F_0-ATPases and pyrophosphatases respectively. The activity of solubilized enzyme was measured in the presence of 0.1–0.5 mg/ml $C_{12}E_8$. The Ca^{2+} and enzyme concentrations were as indicated in the legends to figures.

In addition to the NADH assay we measured ATP hydrolysis from the formation of inorganic phosphate by a colorimetric malachite green method (20). This was done because we found LMCA1 to have an unusually high pH optimum unsuitable for maintaining the stability of the coupled enzyme system involved in the NADH assay. P_i formation was followed as a function of time from the absorbance at 630 nm on a Victor3 (Perkin Elmer) plate reader. Typically, a suboptimal concentration of Ca^{2+} and ATP was used (300 μM $CaCl_2$ and 0.1–0.5 mM ATP) to avoid precipitation of calcium phosphate.

Preparation of Proteoliposomes—LMCA1 was reconstituted with Bio-beads according to (21–23) by incorporation into phospholipid/detergent complexes formed by mixing β-octylglycoside (β-OG) with unilamellar vesicles of dioleoyl phosphatidylcholine (DOPC), prepared by cholate dialysis (24). The protocol for detergent removal by Bio-Beads treatment was the following: 80 mg/ml for 2 h and 1 h, followed by 160 mg/ml twice for 1 h, added to a medium containing β-OG (~15 mg/ml according to titration), liposomes (~9 mg/ml as determined by the diphenylhexatriene method (25)), ~0.4–0.5 mg/ml purified protein and 100 mM KH_2PO_4, 1 mM $MgCl_2$, and 1 mM NaN_3 to which had been added ~17% glycerol. The presence of glycerol was critical for tightness of the vesicles and activity of the protein. Ca^{2+} uptake was measured from the uptake of radiolabeled $^{45}Ca^{2+}$ by use of cellulose nitrate filters (Schleicher & Schuell) (21) in 10% glycerol, 30 mM bis-Tris propane, 150 mM KCl, 1 mM $MgCl_2$, 0.2 mM ATP, 300 μM EGTA, 367 μM Ca^{2+} within 2–3 days (refrigerator stored proteoliposomes), while H^+ release and membrane potential assays were performed on the same day that the vesicles were prepared.

Investigation of H^+ Transport in Pyranine-containing Vesicles—pH changes within the vesicles upon Ca^{2+}-dependent H^+ uptake was followed as a change in the fluorescence of intravesicular pyranine with a Spex Fluorolog-3 spectro-

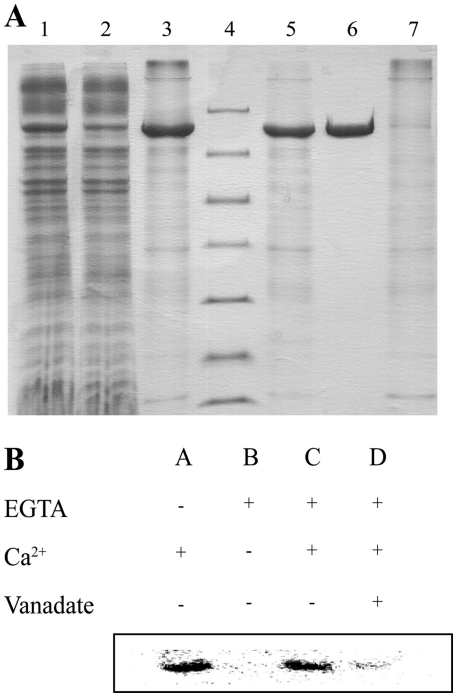

FIGURE 1. *A*, purification of LMCA1. *1–3*, first Ni^{2+} column 1:DDM-solubilized mixed membranes; *2*, flow-through; *3*, imidazole-eluted LMCA1; *4*, marker (116.0, 66.2, 45.0, 35.0, 25.0, 18.4, and 14.4 kDa), *5–7*, second Ni^{2+} column; *5*, TEV protease-digested and dialyzed LMCA1. *6*, flow-through; *7*, imidazole elution; *B*, phosphorylation of LMCA1. The reaction was started by the addition of [γ-^{32}P]ATP and Ca^{2+} resulting in a band corresponding to LMCA1 (*A*). The addition of EGTA, removing Ca^{2+}, abolished the phosphorylation (*B*), but the phosphorylation could be restored by adding back Ca^{2+} (*C*). The phosphorylation could be inhibited by the addition of vanadate (*D*).

fluorometer (excitation wavelength 455 nm, emission wavelength 512 nm, 5 nm slits on both sides). The vesicles were prepared in 7.7 mM KH_2PO_4 pH 7.1, 2.9 mM MOPS pH 7.5 (the remainder from the LMCA1 preparation), 17% glycerol, 90 mM KCl, 0.9 mM $MgCl_2$, 0.8 mM NaN_3, and 0.29 mM pyranine. The extravesicular dye was removed by chromatography on a PD-10 column loaded with reaction buffer (10.6 mM Tris, pH 7.6, 17% glycerol, 90 mM KCl, 0.9 mM $MgCl_2$, 0.8 mM NaN_3). 50 μl of vesicles were added to the 1950-μl reaction buffer under continuous stirring and fluorescence changes induced by additions of ATP, Ca^{2+}, and ionophores were recorded.

Electrogenic Properties of the Enzyme—The formation of transmembrane potentials was followed by oxonol VI fluorescence using a Spex Fluorolog-3 spectrofluorometer (excitation wavelength 580 nm, emission wavelength 660 nm, 10 nm slits on both sides) essentially as previously described (26) and under the same conditions as in the proton release studies.

RESULTS

In this study we have cloned and heterologously overexpressed a putative Ca^{2+}-pump from *L. monocytogenes* (locus tag: *lmo0841*) in *Escherichia coli*. The ATPase was well expressed, resulting in a prominent band on a SDS-PAGE gel from the solubilized membranes (Fig. 1*A*). The two-step metal affinity chromatography procedure on Ni^{2+}-beads yielded highly pure and active enzyme (Fig. 1*A*). The hallmark of P-type ATPase is the formation of a phosphoenzyme intermediate, which we identified by phosphorylation with [γ-^{32}P]ATP in the presence of Ca^{2+} (*lane A*, Fig. 1*B*). The formation of the intermediate was dependent on Ca^{2+}, as the addition of EGTA abolished the phosphorylation (*lane B*, Fig. 1*B*), and the activity could be restored, adding back Ca^{2+} (*lane C*, Fig. 1*B*). Furthermore, phosphorylation could be reduced by the addition of the classical P-type ATPase inhibitor vanadate (*lane D*, Fig. 1*B*).

Classification of LMCA1—Among the five distinct groups of P-type ATPases (3) LMCA1 and a number of other bacterial P-type ATPases belongs to type II Ca^{2+}-ATPases as can be seen from the multiple sequence alignment in supplemental Fig. S1. The alignment shows that essential structural features are conserved, including the presence of 10 transmembrane helices and most of the signature sequences and motifs. Overall the LMCA1 primary structure shows closest sequence identity with the subgroup IIA (sarco(endo)plasmic reticulum Ca^{2+}-ATPases, by 38% identity) and somewhat less pronounced identity (29% identity) to the subgroup IIB (plasma membrane Ca^{2+}-ATPases. A major difference is the presence of inserts of probably regulatory function in the eukaryotic ATPases. This is particularly the case for PMCA, which in addition to the calmodulin-binding C terminus has large inserts, one in the A-M3 linker, and one in the N terminus. But there are also inserts of putative regulatory function in mammalian SERCA-type pumps, *e.g.* the extended luminal loop between M7 and M8, which are not seen in any of the bacterial Ca^{2+}-ATPases. Thus, compared with the 994 residues of rabbit SERCA 1a, LMCA1 is shorter with a total of 880 amino acid residues.

Sequence Analysis and Homology Modeling—With no high-resolution crystal structure of the LMCA1 available, the structure was modeled on the basis of SERCA1a in the Ca^{2+}-bound E1P occluded state (PDB ID 1T5T, see Ref. 25 and Fig. 2*B*). While SERCA1a has two Ca^{2+}-binding sites in the transmembrane region only one of these, corresponding to site II, is conserved in LMCA1 and PMCA (Fig. 2*A* and supplemental Fig. S1). In SERCA1a the Ca^{2+} ion in site I is coordinated by Asp-800, Glu-908, Glu-771, and Thr-799. Asp-800 coordinates both Ca^{2+} ions in SERCA1a and is completely conserved in all Ca^{2+}-ATPases, in contrast to the other three residues that are not conserved in either LMCA1 or PMCA. Importantly, Arg-795 of LMCA1 corresponds to Glu-908 in SERCA1a and a glutamine residue in PMCA (10, 27), see Fig. 2*B*.

Ion Specificity—Considering the above-described differences in the ion-binding site region, it was not entirely clear whether LMCA1 is a genuine Ca^{2+}-ATPase. However, we found that LMCA1 indeed displays a Ca^{2+}-dependent ATP hydrolysis, (Fig. 3*A*). Apart from Ca^{2+}, the only other ion that stimulated ATPase activity (at 50–5000 μM and pH 7.6 or 9) was Sr^{2+}, which is indeed chemically closely related to Ca^{2+}. This is a typical feature of the type IIA subgroup to which the SERCAs belong: unlike PMCA pumps they are capable of transporting Sr^{2+} in addition to Ca^{2+} (28, 29). On the other hand, it is also noteworthy that unlike SERCA1a (30), LMCA1 does not show Mn^{2+}-dependent ATPase activity. Furthermore, we found that Al^{3+}, Ba^{2+}, Co^{2+}, Cs^{+}, Cu^{2+}, $Fe^{2+/3+}$,

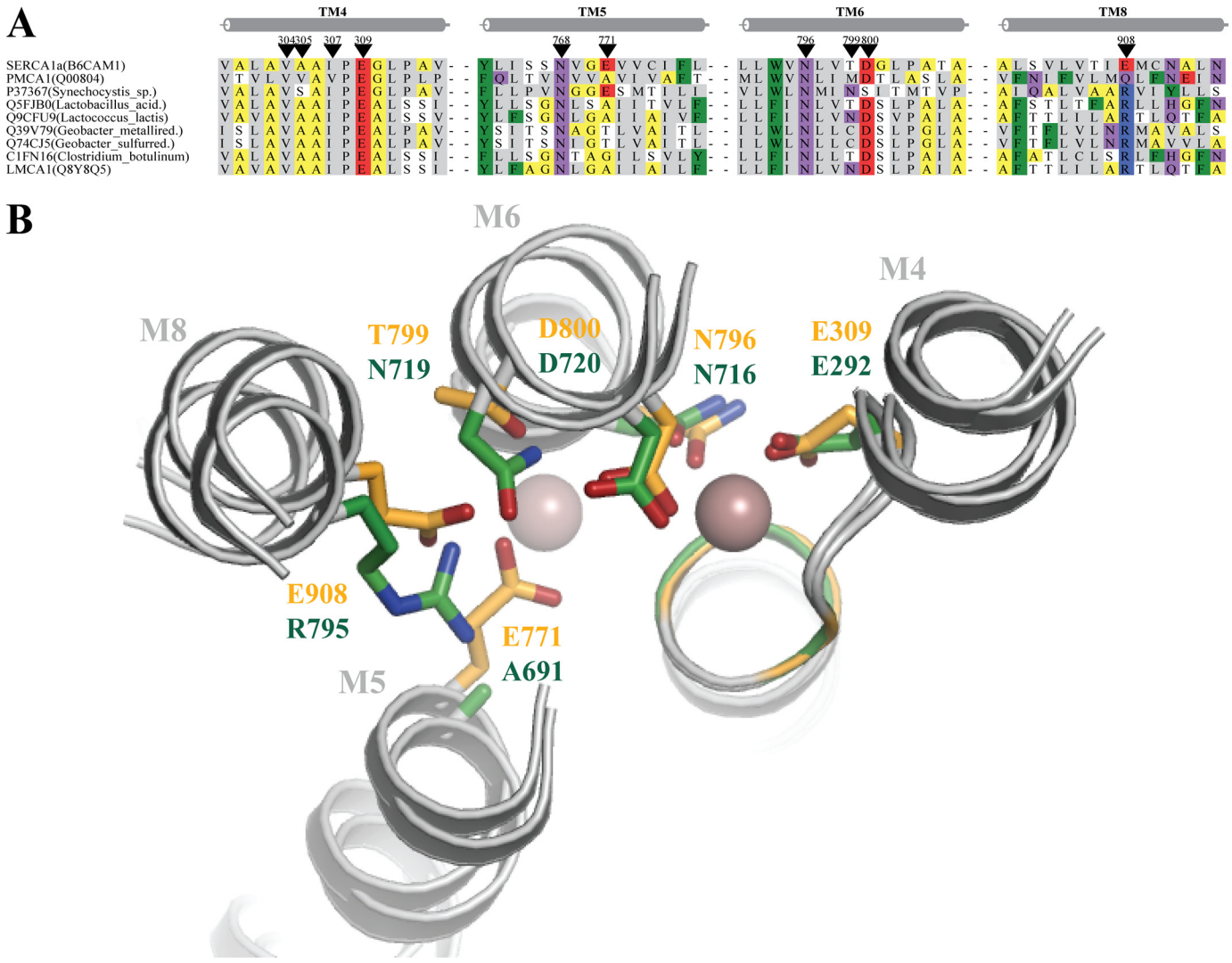

FIGURE 2. *A*, multiple alignment of selected Ca^{2+}-ATPases from rabbit and eubacteria generated by MUSCLE (45). *Black arrowheads* indicate the residues in Ca^{2+}-binding sites I and II of SERCA1a from rabbit. The bacterial sequences were initially identified using PSI-BLAST and a subset of the identified sequences where used to build a Hidden Markov Model profile to search for additional target sequences. The structural elements of transmembrane helices 4, 5, 6, and 8 (TM4, TM5, TM6, and TM8) of SERCA1a (PDB: 1STT) (42) are depicted above the alignment in *gray*. Sequences have less than 85% sequence identity and only two representatives from each bacterial species are presented. The following amino acid groupings are indicated by color schemes: positively charged (*RK*) shown on *blue background*; polar (*QN*) shown in *purple*; hydrophobic (*CLIVM*) with *gray background*; aromatic (*FWY*) with *green background*; small (*TS*) with a *white background*; and tiny (*AG*) with *yellow background*. *B*, homology model of LMCA1 using SERCA 1a in the calcium-bound E1~P.ADP state as a template (PDB: 1T5T) (42). The side chains of SERCA1a are displayed in *yellow* and those of LMCA1 in *green*. The spheres are Ca^{2+} ions from the SERCA1a structure, to the left site I and to the right site II. The transmembrane helices are denoted with M4, M5, M6, and M8 according to SERCA1a.

Li^+, Na^+, and Ni^{2+} did not activate the pump and the addition of Cd^{2+}, Ag^{2+}, and Zn^{2+} inhibited the Ca^{2+}-dependent hydrolysis of ATP (not shown).

Activity of LMCA1 as a Function of Ca^{2+} Concentration—To investigate the apparent Ca^{2+} affinity we studied the hydrolysis of ATP by $C_{12}E_8$-solubilized LMCA1 as a function of Ca^{2+} concentration at a high concentration of the nucleotide (5.0 mM) and pH 7.5 (Fig. 3*B*). However, unlike eukaryotic Ca^{2+}-ATPases we did not detect activity in the submicromolar region. Noticeable activity required a Ca^{2+} concentration of ~10 μM from which level the activity rose steadily to a peak value at 500 μM followed by a marked decrease at higher Ca^{2+} concentrations. As in the case of eukaryotic Ca^{2+}-ATPases the decrease in activity probably can be attributed to a combination of Ca^{2+} binding at low affinity luminal sites and the substitution of the catalytic Mg^{2+} with Ca^{2+} slowing the E1~P:Ca_2 → E2-P transition in SERCA1a (31) and PMCA1 (19, 32). Thus, compared with the eukaryotic Ca^{2+}-ATPases the plots of Ca^{2+} dependence have the same shape, but are shifted toward lower Ca^{2+} affinity by approximately two orders of magnitude. Thus, while for detergent-solubilized SERCA1a $K_{0.5}$ is <1 μM at pH 7.5 (19), the half-maximal activation for LMCA1 was found to be ~80 μM (pH 7.5). For SERCA1a the maximal activity is typically ~5 μmol ATP/(min mg protein) at neutral pH and 20–25 °C (19). For LMCA1 activities as high as ~20 μmol of ATP/(mg protein × min) were observed in detergent solution at pH 7.5 and room temperature, and an even higher activity was seen at pH 9. In conclusion the maximal turnover of LMCA1 is much higher, but characterized by a lower affinity for Ca^{2+} than SERCA1a.

The Dependence of the Activity on pH in Detergent Solution—Our further experiments with LMCA1 solubilized in $C_{12}E_8$

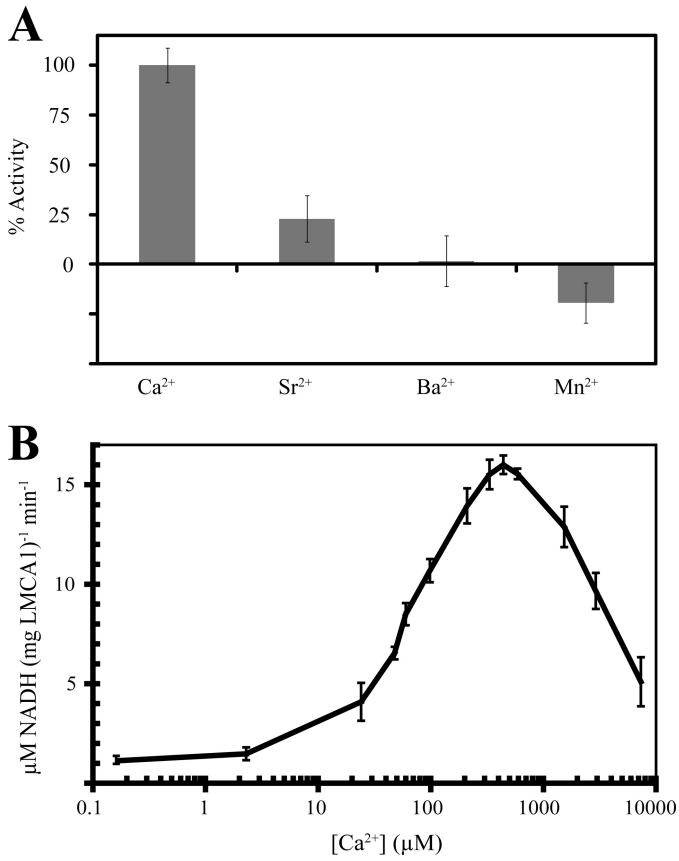

FIGURE 3. *A*, ATPase activity of LMCA1 in the presence of either 200 μM Ca^{2+}, Sr^{2+}, Ba^{2+}, or Mn^{2+} at pH 9. *B*, ATPase activity of LMCA1 as a function of Ca^{2+} concentration measured at pH 7.5.

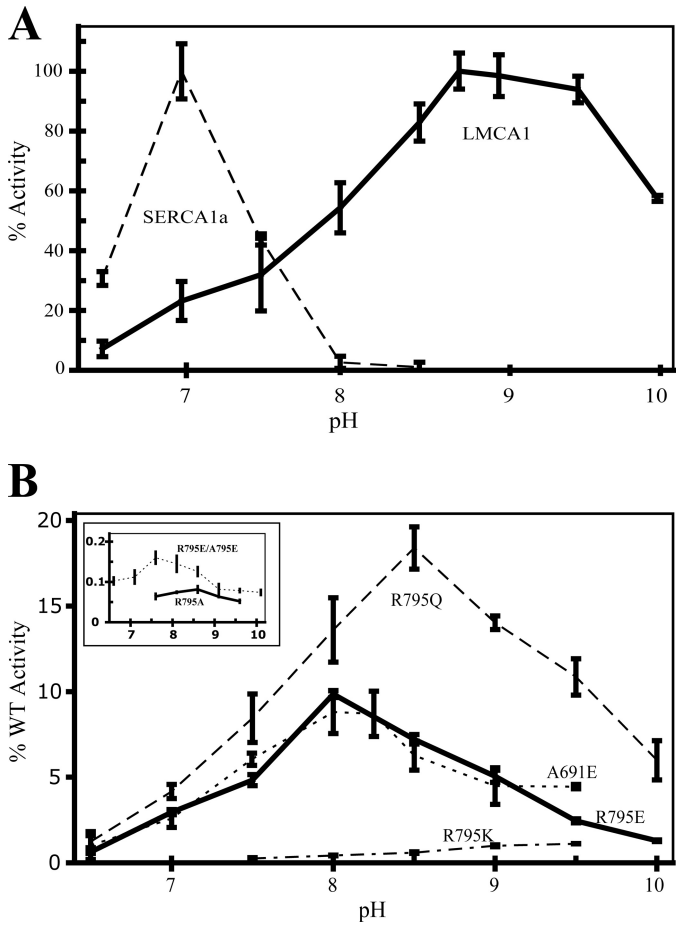

FIGURE 4. **The ATPase activities are depicted as a function of pH in the range 6–10.** *A*, ATPase activity of SERCA1a (*dashed line*) and LMCA1 wild type (*full line*). *B*, ATPase activities of LMCA1 mutant enzymes. R795Q *dashed line*, R795E *full line*, A691E *dotted line*, and R795K *dash-dot line*. The *inset* shows two mutants displaying less than 1% activity: R795A (*full line*) and the double mutant R795E/A795E (*dotted line*). The activity is shown as percentage of wild type activity and scaled according to measurements on fresh protein (the same day as purified) at pH 7.5.

also displayed a very different pH-dependence as compared with SERCA1a and PMCA1. As can be seen in Fig. 4*A*, LMCA1 is active over a broad pH range from 6.5 to 10. The activity rises gradually until pH ~8.75 and remains almost at the same level until the pH reaches 9.5, above which it drops. This is a much broader pH optimum than observed for SERCA1a, for which the activity in the same assay rises gradually from pH 5.5, to reach a maximum at ~pH 7, and then drops steeply to be barely active above pH 8.0. Thus, LMCA1 has a relatively low activity at the pH where SERCA1a has the highest activity while SERCA1a is essentially inactive at the pH where LMCA1 displays its highest activity.

Apparent Ca^{2+} Affinity as a Function of pH—In SERCA1a the Ca^{2+} affinity is strongly pH-dependent as four of the ion-binding residues are carboxylates and their degree of protonation is pivotal for Ca^{2+} coordination. To investigate the pH-dependence of the Ca^{2+} affinity in LMCA1 we studied the activity as a function of the Ca^{2+} concentration at pH 7 and 9 (supplemental Fig. S2). In LMCA1 the apparent affinity was about twice as high at pH 9 as compared with that at pH 7, while a 10-fold increase in affinity was observed with SERCA1a when pH was raised from 6 to 7 (33).

Ca^{2+} Transport: Stoichiometry and pH Dependence—To further investigate the properties of LMCA1 we reconstituted purified LMCA1 in DOPC vesicles to measure the uptake of radioactively labeled Ca^{2+} ($^{45}Ca^{2+}$). As can be seen from Fig. 5*A* LMCA1 did indeed display an ATP-dependent Ca^{2+} uptake. The Ca^{2+} transport displayed a similar pH dependence as the ATPase activity and the initial rate of Ca^{2+} uptake was much higher at pH 9 as compared with 7.6. As can be seen in Fig. 5*B*, the rate of Ca^{2+} uptake was highest initially (as was ATP hydrolysis) and then slowed down with the formation of a transmembrane Ca^{2+} gradient. Comparing the initial rates of Ca^{2+} uptake and enzymatic hydrolysis indicated that the stoichiometry of Ca^{2+} transport and ATP consumption is close to unity (Fig. 5*B*), lower than the values approaching 1.5–2:1 previously found for SERCA1a (34–36). On the other hand, it is similar to the presumed 1:1 Ca^{2+}/ATP stoichiometry for PMCA (13).

Mutational Studies—The most striking difference between the ion-binding sites of LMCA1 and SERCA1a is the absence of two glutamates coordinating Ca^{2+} at site I in SERCA1a (Glu-771 and Glu-908). As explained above, LMCA1 is a member of a large group of bacterial proteins with an arginine in one of these positions (908, SERCA numbering) while PMCA has a glutamine in this position. To investigate whether the presence of the arginine could explain the observed biochemical differences we expressed and purified a

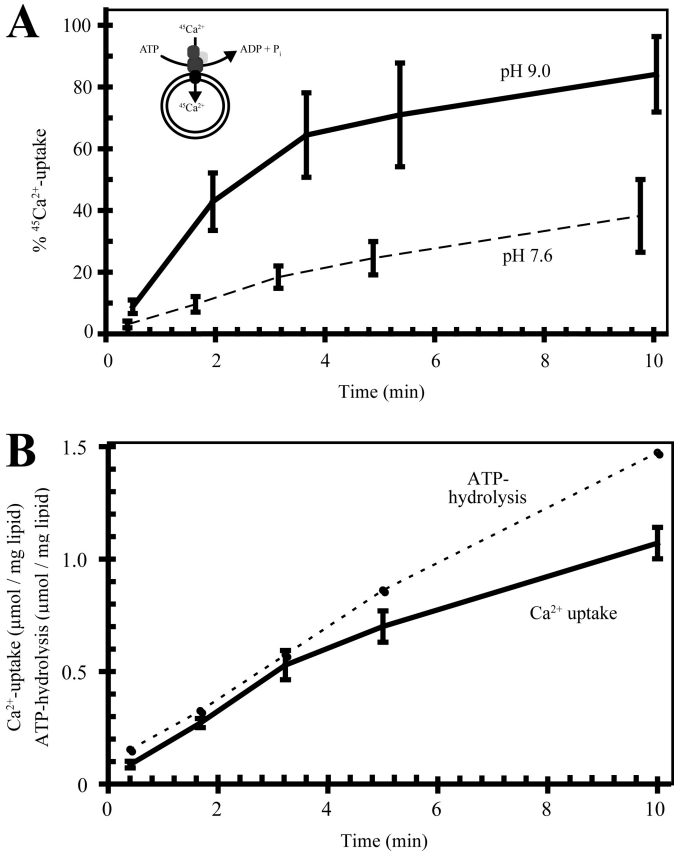

FIGURE 5. **Uptake of $^{45}Ca^{2+}$ into DOPC vesicles.** *A*, percentage of maximal uptake at pH 7.6 (*dashed line*) and 9.0 (*full line*). *B*, a comparison of Ca^{2+} uptake (μM Ca^{2+}/mg lipid/ml) and ATPase activity (μmol ATP/mg lipid) at pH 7.6.

mutant LMCA1 carrying a glutamate in this position, as in SERCA1a (R795E). Interestingly, we found by this mutation that the pH optimum was shifted by 1 pH unit toward that of SERCA1a (pH 8.0), see Fig. 4*B*.

We then constructed a mutant having a glutamine in position 795 as in PMCA. Interestingly the pH optimum of this mutant, carrying a neutral residue in position 795, had a pH optimum of ~8.5, intermediate of the positively charged arginine in the wild-type protein and the negatively charged glutamate in R795E (Fig. 4*B*). Note that both LMCA1 and PMCA have an alanine in position 691 where SERCA1a has Glu-771 (see supplemental Fig. S1). Thus both residues (691 and 795 in LMCA1 numbering) are similar in the R795Q mutant and PMCA. Despite this similarity PMCAs typically seem to have a lower pH optimum (37) than the R795Q mutant of LMCA1.

We also introduced a glutamate at Ala-691 of LMCA1, corresponding to the ion binding residue Glu-771 in SERCA1a. In this A691E mutant of LMCA1 the pH optimum was 8, as in the R795E mutant enzyme (Fig. 4*B*). Thus, the introduction of either of the two ion-binding glutamates specific for SERCA shifted the pH dependence of LMCA1 in a similar way.

Three more mutants were constructed (R795K, R795A, and the R795E/A691E double mutant). Although they had very low activity (<1% of wild type), making the significance of the results more uncertain, these mutants displayed a similar tendency with regard to pH dependence, as observed with the above-described mutants. Thus, the charged-conservative R795K mutant displayed a similar pH dependence as the wild type. The double mutant (R795E/A691E), mimicking SERCA1a, had a similar pH dependence as SERCA1a and the behavior of the R795A mutant was reminiscent of the R795Q mutant that also carries a non-charged residue in this position.

Surprisingly, the Ca^{2+} affinity of all mutants was even lower than that of the wild type (not shown). Thus, it was not possible to restore the Ca^{2+} binding properties by mimicking the ion-binding site I of SERCA1a alone.

LMCA1 and Proton Flux—In SERCA1a the influx of 2 Ca^{2+} per ATP is coupled to extrusion of 2–3 H^+, where the stoichiometry varies with pH (26, 35, 38, 39). For PMCA 1 Ca^{2+} and probably 1 H^+ are translocated in each cycle (13), although a higher H^+ stoichiometry has also been reported (40, 41). In contrast, no evidence of a counter ion or electrogenecity has been demonstrated previously for bacterial P-type ATPases. To resolve this issue, we investigated LMCA1 reconstituted in DOPC vesicles loaded with the pH-sensitive fluorescent dye pyranine (Fig. 6). In this figure, a decrease in fluorescence reflects a decrease in pH inside the vesicle. When the membrane potential is clamped by addition of valinomycin, a slow proton transport is revealed, probably due to a small difference in the inside and outside pH values. The fact, that this decrease in pH was induced by valinomycin can be attributed to the formation of a positive inside membrane potential hindering the passive influx of protons. The following addition of 100 μM Ca^{2+} does not affect the passive proton transport as seen from the unchanged velocity of the fluorescence decrease. However, the subsequent addition of 1.0 mM ATP reverses the fluorescence change, *i.e.* induces an ATP-dependent efflux of protons. The *inset* in Fig. 6 demonstrates that Ca^{2+} is absolutely necessary for initiation of the ATP-dependent efflux, because it is completely abolished by addition of EGTA (a Ca^{2+}-chelating agent). Taken together, these experiments demonstrate that in the reconstituted vesicles LMCA1 exchanges H^+ for Ca^{2+} ions by an ATP-dependent transport process. Thus ATP addition allows maintaining a steady state concentration gradient of H^+. The ionophore A23187 abolishes the transmembrane Ca^{2+} gradient (built up by LMCA1) and induces an instantaneous fall in pyranine fluorescence, indicative of re-uptake of protons, since the ionophore exchanges 2 H^+ for 1 Ca^{2+}. However, subsequently there is a slow, time-resolved decrease in pyranine fluorescence, which is, at first sight, surprising since it indicates a sustained net transport of the protons into the vesicles. This observation is, however, crucial for resolving the question about the stoichiometry of H^+/Ca^{2+} exchange ratio. The net transport of Ca^{2+} under these conditions is zero (Ca^{2+} influx induced by the pump is equal to the Ca^{2+} efflux through A23187). Furthermore, active Ca^{2+} transport by LMCA1 is coupled to H^+ translocation in the opposite (outwards) direction. Because a net inwards transport of H^+ is seen, this must mean that H^+ translocation by the ionophore and LMCA1 take place with a different stoichiometry and in such a way that H^+/Ca^{2+} exchange ratio by LMCA1 is lower than the 2:1 stoichiometry for A23187. Thus, LMCA1 is likely to catalyze a Ca^{2+}/H^+

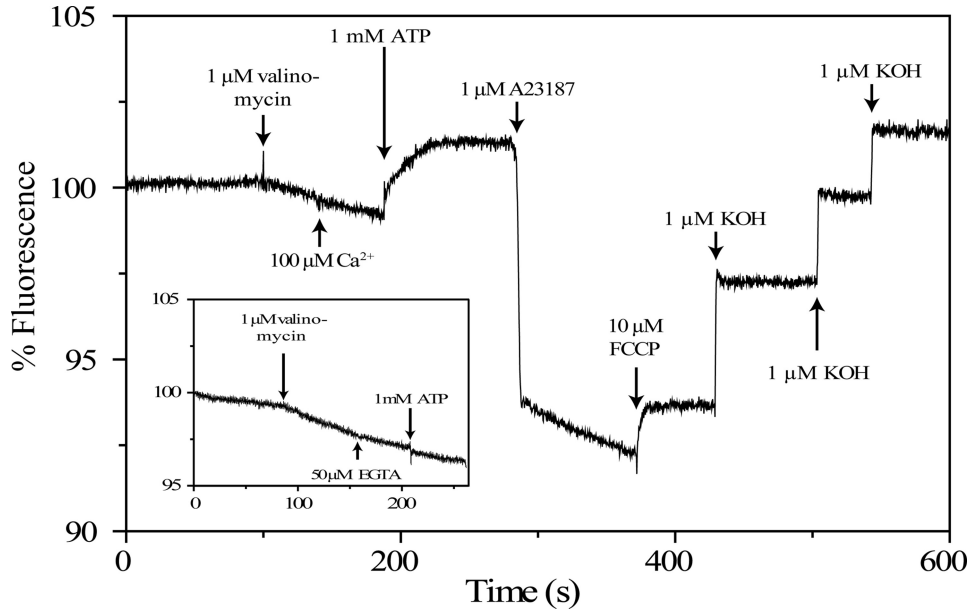

FIGURE 6. **Transport and electrogenic properties of LMCA1 resonstituted in DOPC vesicles.** H^+ transport measured with the pH-sensitive fluorescent dye pyranine. Changes in fluorescence are corrected for dilution. The addition of the various compounds is marked by *arrows*.

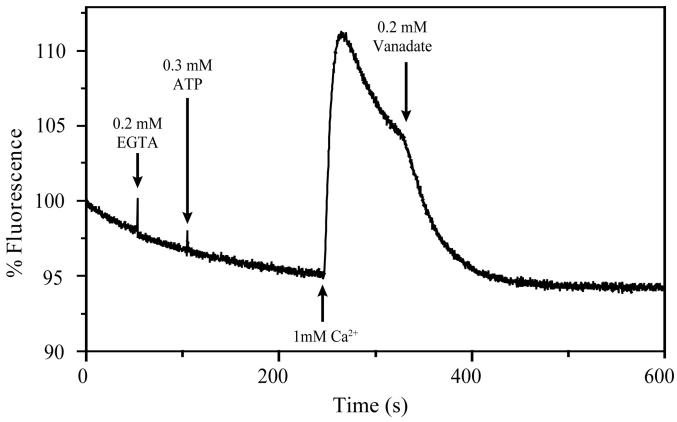

FIGURE 7. **Changes in the transmembrane potential reported by oxonol fluorescence.** Addition of ATP and Ca^{2+} to LMCA1 reconstituted in DOPC vesicles builds up the membrane potential. Vanadate inhibits LMCA1 and leads to dissipation of the membrane potential.

exchange reaction with a ratio of $1Ca^{2+}$:$1H^+$, which implies that it is an electrogenic process.

Electrogenic Properties of LMCA1—To substantiate the above conclusion we have further investigated the electrogenecity of the LMCA1 catalyzed Ca^{2+} transport process with oxonol VI. An increase in the fluorescence of this dye corresponds to the formation of a positive inside membrane potential. Fig. 7 clearly demonstrates that net transport of positive charges takes place into the liposomes containing reconstituted enzyme. The potential is dependent on the simultaneous presence of ATP and Ca^{2+}, and it is inhibited by vanadate. Because we have now shown that LMCA1 exchanges Ca^{2+} for H^+ and during this process builds up a positive inside membrane potential, the stoichiometry is probably $1Ca^{2+}$:$1H^+$ in accordance with the pyranine data.

DISCUSSION

Classification of LMCA1—The present study firmly establishes that the gene locus *lmo0841* in *L. monocytogenes* encodes a Ca^{2+}-ATPase and hence we name it LMCA1. Overall it shares highest sequence similarity with SERCA-type ATPases but also to some extent with those ATPases of the PMCA-type. LMCA1 differs from both by having an arginine in a position that in sequence alignments is equivalent to Glu-908 in SERCA1a and Gln-983 in PMCA1 (supplemental Fig. S1). We have found this arginine to be characteristic of a large group of bacterial Ca^{2+}-ATPases (Fig. 2*A*). The position equivalent to Glu-771 in SERCA is furthermore occupied by an alanine in a large fraction of this group, reminiscent of the PMCA type pumps. Because of these differences to SERCA, LMCA1 has only one ion-binding site, which in accordance with our findings is able to transport one Ca^{2+} and countertransport one H^+ by an electrogenic mechanism. In other respects there are marked differences from both SERCA and PMCA, *e.g.* LMCA1 has a low Ca^{2+} affinity and a high pH optimum.

The Minimal Subset of Amino Acids Required for Ca^{2+} Pumping—We have in Fig. 2*B* modeled the LMCA1 sequence on the structure of SERCA1a in the occluded Ca_2E1P:ADP state (represented by the Ca_2E1:AlF_4^-:ADP complex, PDB ID 1T5T) (42). Interestingly, our homology model indicates that the guanidinium group of Arg-795 in LMCA1 (corresponding to the SERCA Glu-908 position) might exploit a position in space close to the Glu-771 side chain of SERCA1a, which is replaced by the small Ala-691 in LMCA1 (Fig. 2*B*). Indeed the arginine replacing Glu-908 in SERCA1a in a large subset of this group of bacterial Ca^{2+}-ATPases is highly correlated with a small residue (Ala or Gly) in the position corresponding to SERCA 1a Glu-771 (Fig. 2*A* and supplemental Fig. S1). However, it should be noted that an equally large group of putative bacterial Ca^{2+}-ATPases retains the Glu-771 of SERCA1a, suggesting that they might accommodate the arginine differently and possibly display different characteristics of Ca^{2+} binding and pH dependence.

Putatively Conserved Mechanism—We note that the residues that are most dramatically reorientated when shifting between E1 and E2 states in SERCA1a (Glu-309, Asn-796, and Asp-800) (43) and thus important for the shift between high and low affinity for Ca^{2+}, are all conserved in LMCA1 (Fig. 2*A*). Thus, although site I is disrupted in LMCA1, the important residues involved in the Ca^{2+}-pumping mechanism at site II are conserved, consistent with the view that they likely represent the minimal requirement for Ca^{2+}/H^+ exchange over the membrane by P-type Ca^{2+}-ATPases.

The pH Dependence of LMCA1—As it is known that the *lmo0841* gene is up-regulated at high pH (9.5) (15), it was also for this reason interesting to investigate the pH dependence of the protein. The activity of detergent-solubilized LMCA1 displayed optimal activity near pH 9.0 (Fig. 4*A*). Moreover, the Ca^{2+} uptake in reconstituted vesicles was faster at pH 9 than at pH 7.6 (Fig. 5*A*), thus correlating an increased ATP hydrolysis with increased transport activity. Our mutational studies indicate that the pH optimum of the wild-type enzyme probably is tuned by the charge of the arginine in position 795. The activity displays a broad plateau in the pH region 8.75–9.75. This plateau might indicate that activity is dependent on two different rate-limiting events connected to the pK_a of two different amino acid residues. Because the peak at 9.75 seems to disappear in the R795Q (and R795A) mutants, this would be consistent with a mechanism where the activity peak at pH ~9.75 would be related to deprotonation of Arg-795. The importance of the positions 795 and 691 is further supported by another Ca^{2+}-ATPase from *Synechosystis sp.* It has the same constellation of amino acids as the A691E mutant LMCA1, viz. an arginine in position 795 and a glutamate in position 691 (LMCA1 numbering) and a similar pH optimum (~8) as the LMCA1 mutant (6). However, PMCAs seem to have a lower pH optimum than the R795Q-mutant of LMCA1, which mimics PMCA in these positions. This might be explained by the presence of yet another glutamate in the transmembrane region of PMCA1 (Glu-987) that is not seen in SERCA1a or the bacterial ATPases (supplemental Fig. S1).

To address the transport mechanism we modeled LMCA1 on the structure of SERCA1 in the open E2P ground state (represented by the E2:BeF_3^- complex, PDB ID 3B9B) (43) (Fig. 8). In this model not only Glu-292 and Asn-716 (corresponding to Glu-309 and Asn-796 in SERCA 1a), but also Arg-795 in LMCA1 (instead of Glu-771 in SERCA 1a) has direct contact with the broad channel that opens up toward the extracytosolic side when Ca^{2+} is released and H^+ taken up. Consequently, Arg-795, when protonated might repel incoming H^+, thereby preventing efficient pumping at lower or neutral pH. That an arginine would sense the pH on the outside rather than on the cytosolic side is also more probable from a physiological point of view, since the cytosol would not be expected to reach pH 9 at any point.

A further and related molecular explanation for the unusually high pH optimum of LMCA1 as compared with SERCA1a is based on the different charges in and near the ion-binding sites in the E1 conformations of the different Ca^{2+}-ATPases. The LMCA1 ion-binding site contains two carboxylate sidechains that when deprotonated will compensate for the charge of an incoming Ca^{2+} ion (Fig. 2*A* and supplemental Fig. S1). However, at neutral pH Arg-795 of LMCA1 is likely to remain in a protonated state. Thus, with one Ca^{2+} ion bound, the ion-binding site will bear an uncompensated positive charge at neutral pH. Uncompensated charges in the membrane are energetically costly to harbor. Consequently, Ca^{2+} affinity and the activity of this pump is likely to be energetically favored at high pH when Arg-795 is deprotonated. According to the same reasoning as above the four carboxylates present in SERCA will be able to charge compensate the two divalent Ca^{2+} ions translocated by SERCA1a and likewise the two carboxylates in the ion-binding site of PMCA could charge compensate the one Ca^{2+} ion translocated by PMCA. Therefore, in agreement with the mutant data (Fig. 4*B*), introducing an arginine in position 795 is likely to be an efficient means to tune activity toward a high pH optimum according to the pK_a of the arginine for the transport of one Ca^{2+} per cycle.

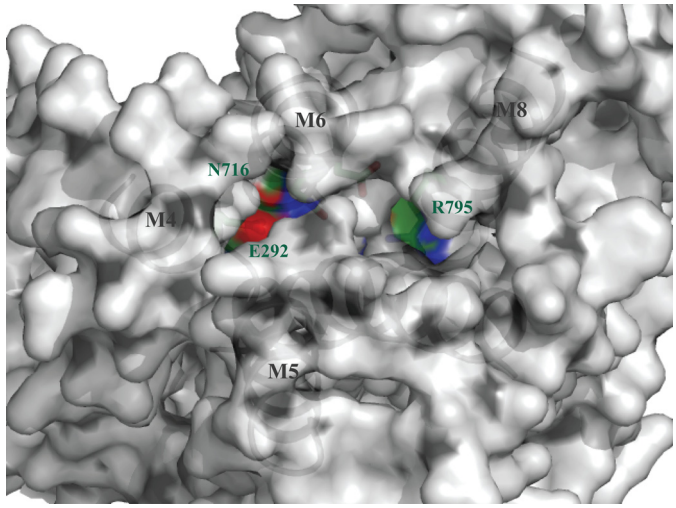

FIGURE 8. **Homology model of LMCA1 generated using SERCA 1a in E2P ground state (PDB: 3B9B) (43) as template.** LMCA1 is viewed from the lumen and reveals Arg-795 situated in an open channel in this state with direct access to the extracellular environment. Carbon, nitrogen, and oxygen atoms are displayed in *green*, *blue*, and *red*, respectively.

Physiological Role—It is noteworthy that *L. monocytogenes* lives and thrives well at pH values as high as 9 or even 10. Attempts to identify LMCA1 as an abundant protein in isolated membranes of the non-pathogenic strain *Listeria innocua* grown either at pH 7 or 9.5 were not conclusive. At the transcriptional level, LMCA1 is up-regulated after adaptation at high pH (15), and it is likely that this pump, being situated in the plasma membrane, facilitates survival of the bacterium when stressed by a combination of a high Ca^{2+} concentration and alkaline pH. The intracellular Ca^{2+} concentration in bacteria is typically regulated by H^+/Ca^{2+} exchangers driven by the proton gradient (2, 44). A reduction, or even reversal, in the proton gradient at high pH may necessitate the use of a primary ATP-driven transporter under these conditions.

The vital importance of keeping Ca^{2+} homeostasis makes Ca^{2+} extruders potentially interesting drug targets. Interestingly it has recently been shown that the survival of the pathogen *Streptococcus pneumoniae* in the high Ca^{2+} concentra-

tions in the extracellular fluid of the human host depends on a SERCA-type Ca^{2+} extruder named CaxP (9).

CONCLUSION

In summary, we have characterized a bacterial SERCA-homologue, LMCA1, at the protein level. Although LMCA1 has a high sequence similarity to, and a similar overall structure as SERCA as shown by homology modeling, we have also found major differences in the biochemical and biophysical properties of the two proteins that to a large extent can be rationalized on the basis of a few crucial differences between the intramembranous charged residues among the different Ca^{2+}-ATPase types. Finally we have established both Ca^{2+} and H^+-transport, with stoichiometries of 1 Ca^{2+} and presumably 1 H^+ per ATP hydrolyzed, revealing LMCA1 as an electrogenic pump.

Acknowledgments—We thank Pascale F. Cossart (Institute Pasteur, Paris, France) for generously providing us with L. monocytogenes genomic DNA. Listeria innocua (serotype 6a, described in Leimeister-Wächter and Chakraborty, Ref. 46) was kindly provided by Jürgen Wehland, Helmholtz Centre for Infection Research, Braunschweig, Germany. We greatly appreciate the excellent technical assistance from: Birte Nielsen, Anna Marie Nielsen, and Karen Marx.

REFERENCES

1. Campbell, A. K. (1983) *Intracellular Calcium: Its Universal Role as Regulator*, John Wiley and Sons, New York
2. Rosen, B. P. (1987) *Biochim. Biophys. Acta* **906,** 101–110
3. Axelsen, K. B., and Palmgren, M. G. (1998) *J. Mol. Evol.* **46,** 84–101
4. Ambudkar, S. V., Lynn, A. R., Maloney, P. C., and Rosen, B. P. (1986) *J. Biol. Chem.* **261,** 15596–15600
5. Geisler, M., Richter, J., and Schumann, J. (1993) *J. Mol. Biol.* **234,** 1284–1289
6. Geisler, M. (1998) *Biol. Proced Online* **1,** 70–80
7. Berkelman, T., Garret-Engele, P., and Hoffman, N. E. (1994) *J. Bacteriol.* **176,** 4430–4436
8. Raeymaekers, L., Wuytack, E., Willems, I., Michiels, C. W., and Wuytack, F. (2002) *Cell Calcium* **32,** 93–103
9. Rosch, J. W., Sublett, J., Gao, G., Wang, Y. D., and Tuomanen, E. I. (2008) *Mol. Microbiol.* **70,** 435–444
10. Toyoshima, C., Nakasako, M., Nomura, H., and Ogawa, H. (2000) *Nature* **405,** 647–655
11. Clarke, D. M., Loo, T. W., Inesi, G., and MacLennan, D. H. (1989) *Nature* **339,** 476–478
12. Andersen, J. P. (1995) *Biosci. Rep.* **15,** 243–261
13. Salvador, J. M., Inesi, G., Rigaud, J. L., and Mata, A. M. (1998) *J. Biol. Chem.* **273,** 18230–18234
14. Guerini, D., Foletti, D., Vellani, F., and Carafoli, E. (1996) *Biochemistry* **35,** 3290–3296
15. Giotis, E. S., Muthaiyan, A., Blair, I. S., Wilkinson, B. J., and McDowell, D. A. (2008) *BMC Microbiol.* **8,** 102
16. Sali, A., and Blundell, T. L. (1993) *J. Mol. Biol.* **234,** 779–815
17. Eswar, N., Webb, B., Marti-Renom, M. A., Madhusudhan, M. S., Eramian, D., Shen, M. Y., Pieper, U., and Sali, A. (2006) *Curr Protoc. Bioinformatics* 5.6.1–5.6.30
18. Möller, J. V., Lenoir, G., Marchand, C., Montigny, C., le Maire, M., Toyoshima, C., Juul, B. S., and Champeil, P. (2002) *J. Biol. Chem.* **277,** 38647–38659
19. Møller, J. V., Lind, K. E., and Andersen, J. P. (1980) *J. Biol. Chem.* **255,** 1912–1920
20. Lanzetta, P. A., Alvarez, L. J., Reinach, P. S., and Candia, O. A. (1979) *Anal. Biochem.* **100,** 95–97
21. Geertsma, E. R., Nik Mahmood, N. A., Schuurman-Wolters, G. K., and Poolman, B. (2008) *Nat. Protoc* **3,** 256–266
22. Rigaud, J. L., Pitard, B., and Levy, D. (1995) *Biochim. Biophys. Acta* **1231,** 223–246
23. Rigaud, J. L., and Lévy, D. (2003) *Methods Enzymol.* **372,** 65–86
24. Heegaard, C. W., le Maire, M., Gulik-Krzywicki, T., and Møller, J. V. (1990) *J. Biol. Chem.* **265,** 12020–12028
25. London, E., and Feligenson, G. W. (1978) *Anal. Biochem.* **88,** 203–211
26. Cornelius, F., and Møller, J. V. (1991) *FEBS Letts.* **284,** 46–50
27. Guerini, D. (1998) *Cell Tissue Res.* **292,** 191–197
28. Mermier, P., and Hasselbach, W. (1976) *Eur. J. Biochem.* **69,** 79–86
29. Berman, M. C., and King, S. B. (1990) *BBA-Biomembranes* **1029,** 235–240
30. Da Costa, A. G., and Madeira, V. M. (1986) *Arch. Biochem. Biophys.* **249,** 199–206
31. Lund, S., and Møller, J. V. (1988) *J. Biol. Chem.* **263,** 1654–1664
32. Preianò, B. S., Guerini, D., and Carafoli, E. (1996) *Biochemistry* **35,** 7946–7953
33. MacLennan, D. H. (1970) *J. Biol. Chem.* **245,** 4508–4518
34. Inesi, G., Kurzmack, M., and Verjovski-Almeida, S. (1978) *Ann. NY Acad. Sci.* **307,** 224–227
35. Meltzer, S., and Berman, M. C. (1984) *J. Biol. Chem.* **259,** 4244–4253
36. Hasselbach, W., and Oetliker, H. (1983) *Annu. Rev. Physiol.* **45,** 325–339
37. Gmaj, P., Zurini, M., Murer, H., and Carafoli, E. (1983) *Eur. J. Biochem.* **136,** 71–76
38. Yu, X., Carroll, S., Rigaud, J. L., and Inesi, G. (1993) *Biophys. J.* **64,** 1232–1242
39. Levy, D., Seigneuret, M., Bluzat, A., and Rigaud, J. L. (1990) *J. Biol. Chem.* **265,** 19524–19534
40. Thomas, R. C. (2009) *J. Physiol.* **587,** 315–327
41. DeSantiago, J., Batlle, D., Khilnani, M., Dedhia, S., Kulczyk, J., Duque, R., Ruiz, J., Pena-Rasgado, C., and Rasgado-Flores, H. (2007) *Front Biosci.* **12,** 4641–4660
42. Sørensen, T. L., Møller, J. V., and Nissen, P. (2004) *Science* **304,** 1672–1675
43. Olesen, C., Picard, M., Winther, A. M., Gyrup, C., Morth, J. P., Oxvig, C., Møller, J. V., and Nissen, P. (2007) *Nature* **450,** 1036–1042
44. Tsuchiya, T., and Rosen, B. P. (1976) *J. Biol. Chem.* **251,** 962–967
45. Edgar, R. C. (2004) *Nucleic Acids Res.* **32,** 1792–1797
46. Leimeister-Wachter, M., and Chakraborty, T. (1989) *Infect. Immun.* **57,** 2350–2357